Coaxially Fed Hexagonal Patch Antenna for C- and X-band Applications with Reduced-Ground Plane

Abhishek Joshi[1†] and **Rahul Singhal**[2], Non-members

ABSTRACT

The consequence of reduced ground plane in a coaxially-fed hexagonal antenna, on impedance and radiation is analyzed and presented here. Measured and simulated impedance results for a designed antenna are compared with the equivalent circuit model in this paper. The reduction in ground plane excited frequencies in upper C-band and lower X-band. The designed hexagonal antenna uses a substrate with a dimension of 32 × 33.5 mm^2 along with a reduced ground plane of area, 10.44 × 24.44 mm^2. The proposed antenna has a 285 MHz and 380 MHz impedance bandwidth in C-band and X-band respectively. The designed antenna with reduced ground plane works well for C-band and X-band applications.

Keywords: Hexagonal Patch Antenna, Coaxial-feed, Reduced Ground, X-band Antenna

1. INTRODUCTION

Hexagonal monopole antennas fed at the edge and the vertex are widely explored at lower mode for recent wireless communication systems [1]. Deshmukh et al. [2] proposed a hexagonal shape microstrip antenna with co-planar waveguide feed, backed by hexagonal slot ground. The two variations in which patches are rotated by 30° are investigated which yields impedance bandwidth of 100% and 108% respectively. An X-band hexagonal shaped microstrip patch antenna with impedance bandwidth ranging from 9.21 GHz to 9.38 GHz was discussed by Das et al. The return loss was improved and the resonant frequency was shifted by introducing slots on the sides of the patch [3]. Hexagonal slots were introduced by Datta et al. to reduce the patch size by about 80.22%; this has been simulated using Method of Moment based software IE3D [4]. Agrawal et al. designed and presented a hexagonal shaped antenna with second iteration fractal for ultra wideband (UWB) application (2.64–6.96 GHz). The ground slot and slit variation were also simulated at 3.8 GHz and 6.5 GHz with a gain of 2.84 dBi and 5.2 dBi respectively [5].

When a thick substrate is used, the bandwidth of patch antenna with probe feed is narrowed by inductance introduced by a probe or coaxial feed [6]. An L-shaped probe was utilized to feed an antenna to produce a conical radiation pattern as reported by Guo et al. The L-probe is used to feed a patch which is used to compensate the probe inductance [7]. The transmission line model (TLM) was utilized by Vishwakarma to theoretically evaluate the series and shunt inductance introduced by the probe and the shorting pin. It was found that the resonant frequencies' ratios are extremely dependent on the location of the shorting pin [8].

The circuit model for different modes of the rectangular antenna was proposed by Mousskhani et al. [9]. The equivalent circuit model is used to model coaxially fed ultra wideband antenna (UWB) with an impedance bandwidth ranging from 3.94 to 10.65 GHz [10].

Tong et al. explored the characteristics of ground plane dimensions and its reduction using simulations to model various cases. The ground plane with minimum dimension was recommended [11]. Octagonal shaped antenna with the reduced ground plane has been fabricated by Norra et al. [12], with an operating bandwidth of 230 MHz. The dumbbell-shaped defected ground structure (DGS) cell effect on the dimension of MSA was presented by Arya et al. and the cavity backed model was utilized in order to enhance the antenna efficiency [13]. The slotted H antenna with a modified ground plane has been designed and analysed by Razali et al. for WiMAX application (2.45 GHz) [14]. The ground perturbation and ground dimension reduction by introducing a slot to enhance the bandwidth has been presented earlier [15].

A coaxially fed hexagonal antenna is designed and presented. The second section of the paper deals with the antenna design. The dimension of the ground plane is changed to study its effect on antenna characteristics. The measured and the simulated results are compared with the antenna's equivalent circuit model in the third section of the paper. Finally, observations based on the results comparison are concluded.

Manuscript received on April 14, 2018 ; revised on June 7, 2019 ; accepted on July 11, 2019.

The authors are with Department of Electrical and Electronics Engineering, Birla Institute of Technology & Science, Pilani, Rajasthan, India, E-mail: abhishek.joshi@pilani.bits-pilani.ac.in[1] and rahulsinghal@pilani.bits-pilani.ac.in[2]

[†]Corresponding author.

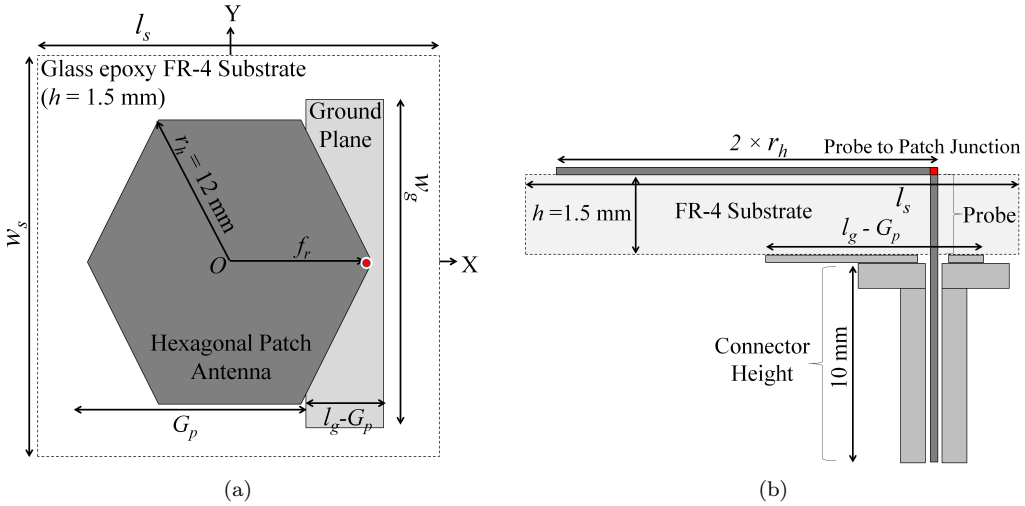

Fig.1: *Schematic of the designed antenna.*

2. ANTENNA GEOMETRY AND PARAMETRIC STUDY

Fig. 1 shows the design of a probe fed hexagonal antenna. The designed antenna in Fig. 1 uses a substrate with a dimension of 32 × 33.5 mm^2. The dimension of the ground plane is 10.44 × 24.44 mm^2. The feed distance from the center of the hexagon f_r is 10 mm. The connector has inner, dielectric and outer radii of 0.805 mm, 2.22 mm and 3 mm respectively, while the connector height is 10 mm.

The dimensions of the antenna's ground plane play a significant role in the antenna's performance. To study the characteristics of ground dimensions, ground plane length is reduced by a factor 'G_p' as shown in Fig. 1. Fig. 2, displays the effect on reflection coefficient by increasing the value of G_p. In all simulations done for parametric analysis, the patch circumradius is 12 mm. It is observed that the resonant frequency can be excited by reducing the ground in a lower frequency of X-band. The patch capacitance (C') is developed due to the patch and the ground being separated by a dielectric material. The resonating frequency is controlled by the capacitance developed by the antenna and the phenomenon of frequency shift can be observed in Fig. 2. The optimum value of 14 mm is chosen for G_p to develop the antenna because of good impedance matching for two bands. The feed location also plays a significant role in impedance matching; to ensure its antenna's sensitivity toward feed location, f_r is varied from 11 to 12.5 mm with steps of 0.5 mm and results are presented in Fig. 3. It can be seen from Fig. 3 that good impedance matching is achieved when the probe is exactly at the vertex of the hexagon, i.e., $f_r = 12.6$ mm.

RLC elements are used to model the designed antenna and equivalent circuit, as shown in Fig. 4. Note that the equivalent circuit model is obtained for the VNA measured resonating frequencies, i.e., 7 GHz (f_1) and 8.69 GHz (f_2) as discussed in the Section 3. The values of lumped elements *RLC* are obtained similarly as done for an E-patch in [10, 16]. After modifying the equations given in [10, 16], Eqs. (1–3) are obtained for a hexagonal patch antenna.

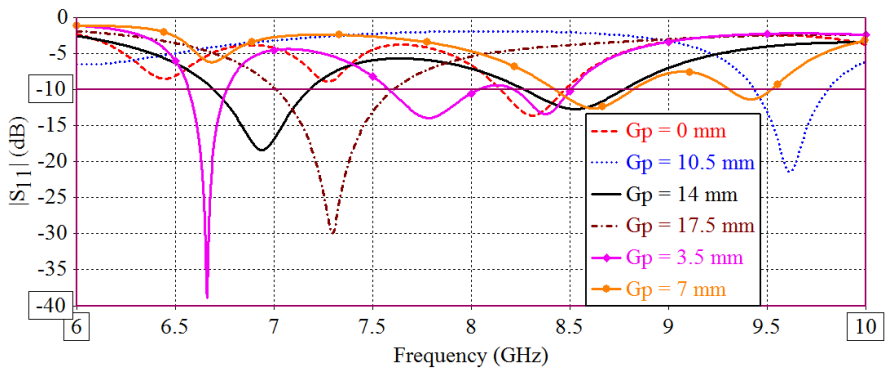

Fig.2: *Reflection coefficients (S_{11}) when G_p varies from 0 mm to 17.5 mm with step of 3.5 mm when f_r = 12.6 mm.*

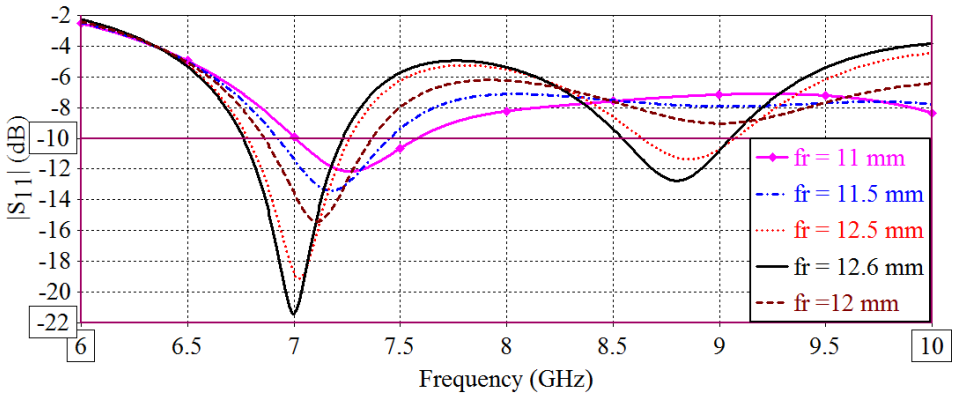

Fig.3: *Simulated S_{11} (dB) of antenna when f_r varies from 11 mm to 12.5 mm with step of 0.5 mm when G_p = 14 mm.*

$$C' = \frac{\varepsilon_o \varepsilon_\varepsilon A_e}{2h} \tag{1}$$

$$l = \frac{1}{(2\pi f_n)C'} \tag{2}$$

$$R = \frac{Q}{(2\pi f_n)C'} \tag{3}$$

where, A_e is patch area over the ground plane. C', C_1 and C_2 are calculated using Eq. (1).

The patch area, $A_e = 374.12$ mm^2 for a full ground and capacitances, $C_1 = C_2 = 4.75$ pF. The patch area, $A_e = 150.03$ mm^2 for reduced ground (G_p = 14 mm) and capacitance, $C' = 1.9$ pF. Due to the reduction in the ground, the value of capacitance of the hexagonal patch is reduced, which is modelled as the series capacitance (ΔC_n). The additional series capacitance of a hexagonal patch can be calculated using the formula given in Eq. (4).

$$\Delta C_n = \frac{C_n \times C'}{C_n - C'} \tag{4}$$

where, n is 1 and 2. The value ($\Delta C_n = 3.18$ pF) of the additional series capacitance of the hexagonal patch using Eq. (4) is indicated in Fig. 4. The hexagonal patch inductance ($L_1 = 0.26$ nH and $L_2 = 0.18$ nH) for 1.5 mm antenna's substrate height (h) and 1.24 mm probe diameter (d) are calculated with Eq. (2) for the frequencies 7.15 GHz (f_1) and 8.69 GHz (f_2) as shown in Fig. 4. Similarly, Eq. (3) is used to find the value of hexagonal patch resistance ($R_1 = 455.16$ Ω and $R_2 = 385.18$ Ω) with $Q = 39.26$ expression available in [17].

Thicker dielectric substrate also increases the inductance in series [6]. The complex probe model is given in [17]. Fig. 4 shows the RLC model of the designed antenna. The input impedance (Z_{11}) of the antenna is evaluated for RLC resonators at resonant frequencies, i.e., 7.15 GHz and 8.69 GHz. The series inductors ($L_o = 0.58$ nH and $L_p = 0.04$ nH) of the SMA connector or feed probe depends on (h). An SMA connector can be modeled by series inductance (L_o and L_p), resistance ($R_p = 37.9$ Ω) and parallel capacitance ($C_o = -0.06$ pF) with other antenna lumped RLC elements. The impedance of the feed can be calculated using the formula given in [17].

In order to distinguish the modes at resonating frequencies, the surface current distributions of the designed antenna are observed at different phases of the excitation signal at the resonating frequencies. The surface current distribution for the proposed antenna is displayed in Figs. 5(a) and (b) at frequencies 7.15 GHz and 8.69 GHz respectively.

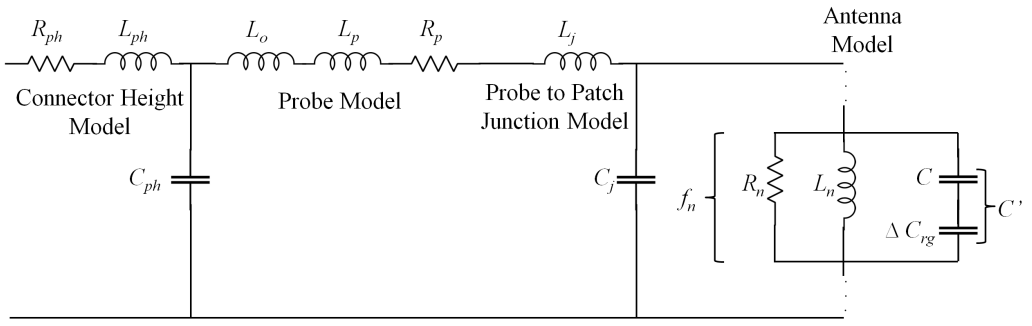

Fig.4: *Circuit model of antenna with its probe feeding network.*

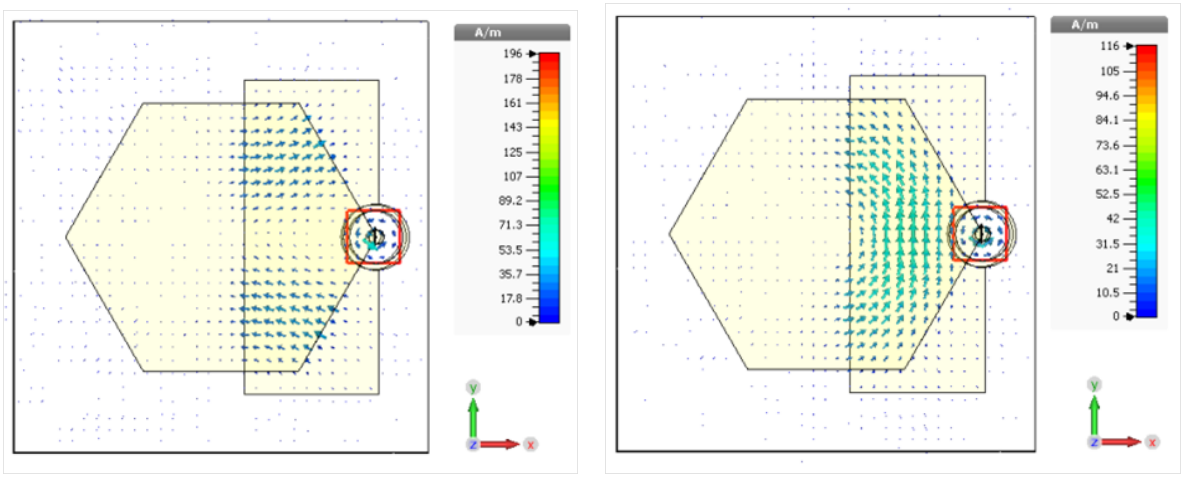

(a) (b)

Fig.5: *Surface current of the designed antennas at (a) 7.15 GHz at 90° phase, (b) 8.69 GHz at 90° phase.*

3. DESIGN EXPERIMENTAL RESULTS AND DISCUSSION

Fig. 6 shows a picture of a developed antenna designed in Section 2. The developed antenna dimensions are 24 × 20.8 mm^2, which is very compact.

The results are obtained using VNA (Keysight N9928A) and compared with the simulated results to study the characteristics of ground plane dimension on reflection coefficient (S_{11}) and impedance (Z_{11}) characteristics for the developed antenna. The equivalent circuit model results are used to compare the reflection coefficient (S_{11}) with simulated and VNA measured results. The simulation results are matching with the measurement when f_r = 12.6 mm, G_p = 14.4 mm, alignment offset of 0.2 mm. While, the equivalent results are close to measurement results, when L_j and C_j are tuned to 0.11 pF and 4.9 nH.

The reflection coefficient S_{11} (in dB), of the antenna, is measured using VNA and is plotted in Fig. 7. Fig. 7 compares the *RLC* model results with feed probe and simulation results using CST MWS. The simulation results show a band from 6.71 to 7.18 GHz (470 MHz) and 8.45 to 8.9 GHz (500 MHz) while VNA measured result shows a band from 6.86 to 7.14 GHz (280 MHz) and 8.41 to 8.79 GHz (380 MHz). The measured VNA bandwidth is less due to the inductance introduced by coaxial feed (SMA connector). The same inductive effect can be verified from VNA measured Smith Chart with a big loop (at 8.69 GHz) in the inductive region shown in Fig. 9(c) while the simulation shows a big loop (8.6 GHz) with a major part in the capacitive region. It proves that the SMA connector is responsible for narrowing down the impedance bandwidth.

The impedance real part and imaginary part are measured and compared with simulated results as presented in Fig. 8 in order to analyse the impedance matching. It is observed that best value of Z_{11} at 8.6 GHz is $49.16 - j27.19\ \Omega$ in the operating band for hexagonal shape using simulated real and imaginary Z_{11} as shown in Fig. 8. Measurements using VNA shows that the value of Z_{11} observed at 8.62 GHz is $50.06 - j18\ \Omega$ in the operating band of the developed antenna, which is quite close to the value mentioned above, i.e., observed during simulations.

The Smith Chart of the designed and developed antennas for 6 to 10 GHz is shown in Fig. 9. In both simulated and measured Smith Chart, a loop is ob-

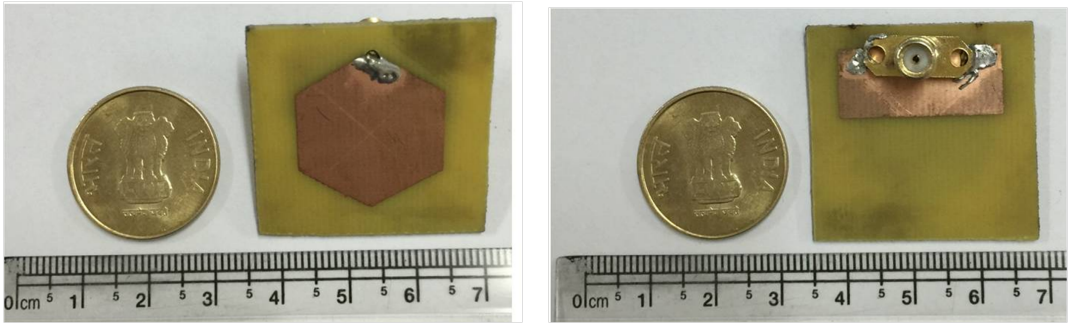

(a) (b)

Fig.6: *Developed antenna (a) top and (b) bottom.*

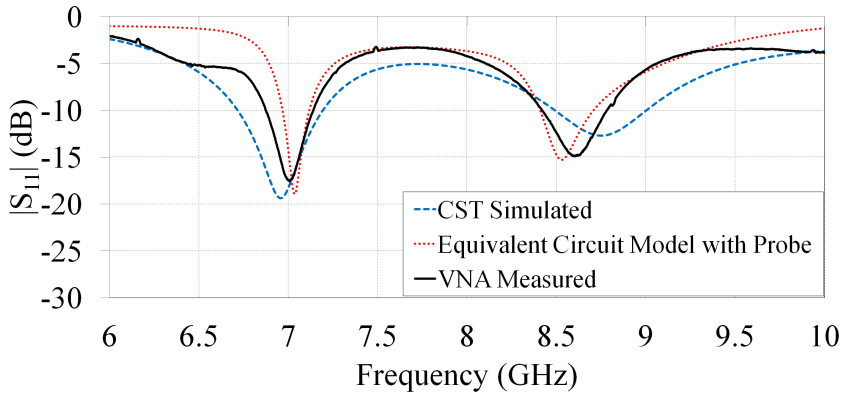

Fig.7: *S_{11} (in dB), reflection coefficient of the antenna.*

served within the operating band as shown in Figs. 9(a) and (b). Simulated results show a large loop in the capacitive region, while the measured results show two loops whose cusps are at 7.15 GHz and at 8.69 GHz frequencies. The Smith Chart for Hexagonal patch antenna with the probe using equivalent circuit model is shown in Fig. 9(b). The junction capacitance (C_j) and inductance (L_j) plays a significant role in input impedance of the antenna as may be depicted from Fig. 9, which shows that the junction between the probe and patch rotates the two loops clockwise in case of measured Smith Chart.

The probe model in CST is less accurate so the maximum portion of the big loop representing the operating bandwidth is present in the capacitive region, i.e., patch reactance dominates the results as shown in Fig. 9(a). Meanwhile, the probe model in equivalent transmission line modelling is more accurate as compared to CST, hence the loop is present in the inductive region as shown in Fig. 9(b). The loop is small and rotated in an anticlockwise direction fully in the inductive region as compared to the equivalent transmission line model.

The radiation patterns of the fabricated probe fed hexagonal antenna are measured with Pre-calibrated standard Dual Ridge Horn (DRH) as shown in Fig. 10(c) in an anechoic environment. The measurement setup involves Agilent E-4412A CW Power Sensor to sense received power and the power is measured by Agilent E-4418B Power Meter while Keysight N5173B RF Signal Generator excites transmitting antenna.

The measured radiation patterns of the hexagonal shaped antenna for frequencies 7 GHz and 8.69 GHz in the XZ-plane (E-plane or Phi = 0° plane) and the YZ-plane (H-plane or Phi = 90° plane) are presented in Figs. 10(a) and (b) respectively. The SMA connector's imperfect position generates a higher order mode and produces a cross-polarization component [17]. The measured boresight gains of the fabricated antenna are 3.7 dB and 2.37 dB respectively at 7 GHz and 8.69 GHz. This is mainly because of the feed located near the vertex of the hexagon and the reduced ground. Moreover, due to reduced ground, the cross-polarization level increases. The W/L ratio is approximately 0.866 which is less than 1 so the patch is supposed to have higher cross-polarization level [17]. Since the W/L value is close to unity, so the cross polarization envelope is overlapping the co-polarization envelope as observed in Fig. 10. To im-

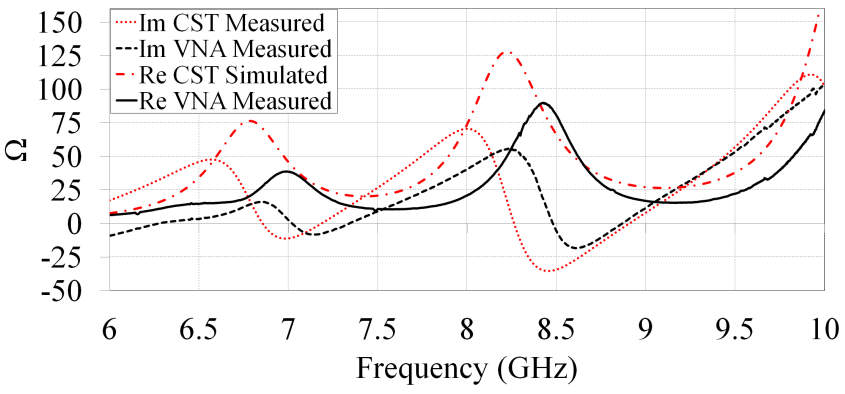

Fig.8: *Measured impedance real and imaginary impedance (Z_{11}).*

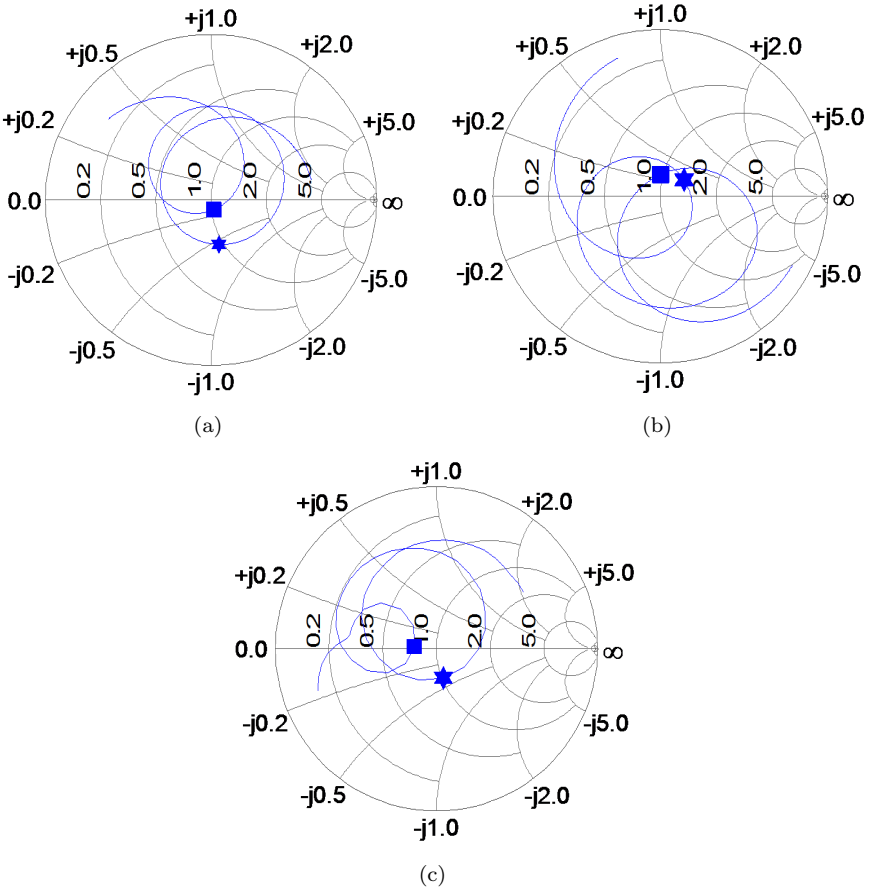

Fig.9: *Antenna Smith Chart (a) CST, (b) RLC Model, and (c) VNA ('■' as 7 GHz and '✶' as 8.6 GHz are indicated.*

prove polarization levels, the aspect ratio of the patch antenna may be altered [17]. C-band and X-band are popularly used in satellite applications but proposed antenna being of moderate gain will be more suitable for line of sight terrestrial communication, e.g., unmanned aerial vehicle-ground link.

4. CONCLUSION

The effect of ground reduction in hexagonal design to achieve X-band lower frequency (8.69 GHz) is studied and analyzed. The ground reduction is achieved by increasing G_p from 0 to 18 mm. The designed antenna impedance bandwidth is narrowed by the introduction of inductance due to direct probe feeding. The input impedance, Z_{11} measured at 7 GHz and 8.69 GHz are $38.6 + j2\ \Omega$ and $50.06 - j18\ \Omega$ respectively. The boresight gain of the designed antenna at 8.35 GHz is 2.91 dB. The radiation patterns do not change with frequency in the operating bandwidth. The antenna proposed in this work has a bandwidth of 285 MHz and 340 MHz at frequencies of C-band and X-band respectively, making it appropriate and affordable for wireless applications.

ACKNOWLEDGMENT

This research work was funded by Department of Science and Technology, New Delhi, India (Reference Number: SR/FST/ETI-346/2013) for equipment.

References

[1] G. Kumar and K.P. Ray ,"*Broadband Microstrip Antenna*," ISBN: 978-1-58053-244-0 Artech House, 2002.

[2] A. Deshmukh, S. Agrawal, K. Lele and K. P. Ray, "Broadband CPW fed Stub loaded hexagonal slot backed hexagonal microstrip antenna," in *2015 International Conference on Microwave and Photonics (ICMAP)*, Dhanbad, 2015, pp. 1-2.

[3] S. Das and S. Gokhroo, "Novel hexagonal pizza shaped CPW microstrip patch antenna for applications in X band," in *2015 Communication, Control and Intelligent Systems (CCIS)*, Mathura, India, 2015, pp. 15-17.

[4] B. Datta, A. Das, A. Kundu, M. Mukherjee and S. K. Chowdhury, "Triple band slotted patch antenna for microwave communication," in *2013 IEEE 3rd International Advance Com-*

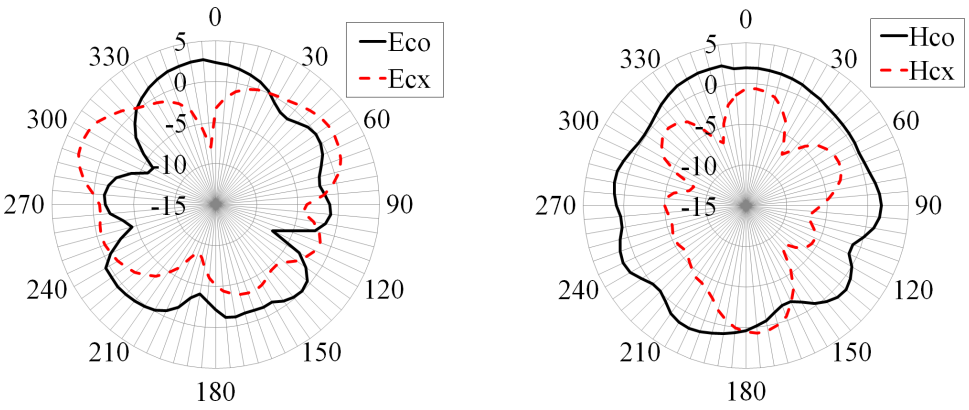

(a)

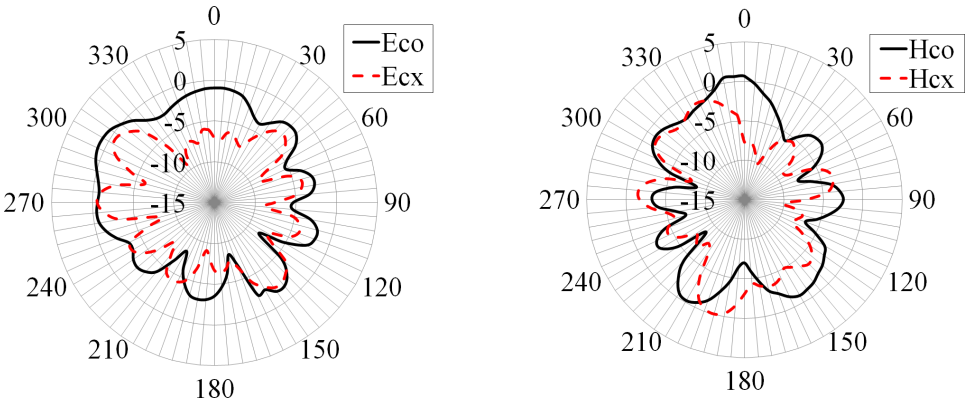

(b)

(c)

Fig.10: *The farfield gain (dB) H-plane (Co and Cross) and E-plane (Co and Cross) respectively measured at (a) 7 GHz, (b) 8.69 GHz, and (c) Measurement setup.*

puting Conference (IACC), Ghaziabad, 2013, pp. 202-206.

[5] S. Agrawal, R. D. Gupta and S. K. Behera, "A hexagonal shaped fractal antenna for UWB application," in *International Conference on Communications, Devices and Intelligent Systems (CODIS)*, Kolkata, 2012, pp. 535-538.

[6] C. A. Balanis, "*Antenna Theory, Analysis and Design*," John Wiley & Sons, New York, 2008.

[7] Yong-Xin Guo, M. Y. W. Chia, Zhi Ning Chen and Kwai-Man Luk, "Wide-band L-probe fed circular patch antenna for conical-pattern radiation," *IEEE Transactions on Antennas and Propagation*, vol. 52, no. 4, pp. 1115-1116, April 2004.

[8] R. K. Vishwakarma, "Rectangular microstrip antenna for dual-band operation," *Applied Electromagnetics Conference (AEMC)*, 2009, Kolkata, 2009, pp. 1-4.

[9] K. Mousskhani and A. Ghorbani, "A modified broadband transmission line model for rectangular patch antennas," in *International Conference on Microwave and Millimeter Wave Technology (ICMMT 2008)*, Nanjing, 2008, pp. 1041-1043.

[10] H. Malekpoor and S. Jam, "Analysis on bandwidth enhancement of compact probe-fed patch antenna with equivalent transmission line model," *IET Microwaves, Antennas & Propagation*, vol. 9, no. 11, pp. 1136-1143, August, 2015.

[11] K. F. Tong, K. F. Lee and K. M. Luk, "On the effect of ground plane size to wideband shorting-wall probe-fed patch antennas," in *2011 IEEE-APS Topical Conference on Antennas and Propagation in Wireless Communications (APWC)*, Torino, 2011, pp. 486-486.

[12] S. R. Norra, A. A. H. Azremi, P. J. Soh, N. A. Saidatul and M. I. Ibrahim, "Small rectangular parasitic plane as patch antenna ground plane for broadband WLAN application," in *Asia-Pacific Conference on Applied Electromagnetics (APACE 2007)*, Melaka, 2007, pp. 1-5.

[13] A. K. Arya, M. V. Kartikeyan and A. Patnaik, "Efficiency enhancement of microstrip patch antenna with defected ground structure," in *International Conference on Recent Advances in Microwave Theory and Applications (MICROWAVE2008)*, Jaipur, 2008, pp. 729-731.

[14] R. Razali, M. Z. A. Abd Aziz, M. K. Suaidi, H. Nornikman and F. Malek, "Modified H-shaped patch antenna with slots and modified ground plane," in *2015 International Conference on Computer, Communications, and Control Technology (I4CT)*, Kuching, 2015, pp. 502-505.

[15] S. Islam and M. Latrach, "Bandwidth enhancement and size reduction of patch antenna by etching linear slots in the ground plane," in *2015 1st URSI Atlantic Radio Science Conference (URSI AT-RASC)*, Gran Canaria, Spain, 2015, pp. 1-1.

[16] A. Joshi and R. Singhal, "Lower Mode Excitation in Vertex-Fed Slotted Hexagonal S-Band Antenna," *AEU - International Journal of Electronics and Communications*, 2018, vol. 87, pp. 180-185.

[17] R. Garg et al., "*Microstrip antenna design handbook*," Artech House Inc; 2001.

Abhishek Joshi received Bachelor's degree in Electronics and Communication Engineering from Rajasthan Technical University, Kota, Rajasthan, India, in 2010 and Master's degree in Digital Communication from Rajasthan Technical University, Kota, Rajasthan, India, in 2013. He is currently working towards the Ph.D. degree in the Department of Electrical and Electronics Engineering, Birla Institute of Technology and Science, Pilani-Campus, Pilani, Rajasthan, India.

His current research interests include different antennas design, wideband microstrip antennas for UWB applications and wireless communication, analysis of antenna with equivalent circuit models, designing the periodic structures such as AMCs, and FSSs, and antenna design with AMC surfaces.

Rahul Singhal received his B.E. in Electronics Engineering from Nagpur University in 1999. Post graduation, he started his teaching career itself. He taught electronics engineering courses for six years in KNMIET, Modinagar. During the tenure, he joined his M.Tech in Digital Communication from Uttar Pradesh Technical University. He received his M.Tech in 2007 and soon after, he got registered in his Ph.D. at Birla Institute of Technology and Science (BITS), Pilani-Campus, Pilani, which he completed in 2013. He is now working as an Assistant Professor in Department of Electrical and Electronics Engineering, BITS, Pilani since 2013. His doctoral work lies in the area of integrated optics involving the design and technology development of various passive photonic components like optical waveguides and power splitters. His present research interest lies in area of planar antenna design and radio over fiber/ FSO network for communication applications. He has authored and co-authored technical papers in various reputed international journals and conferences. He is a member of the IEEE, a fellow of the Optical Society of India and the Institution of Electronics and Telecommunication Engineers (India).